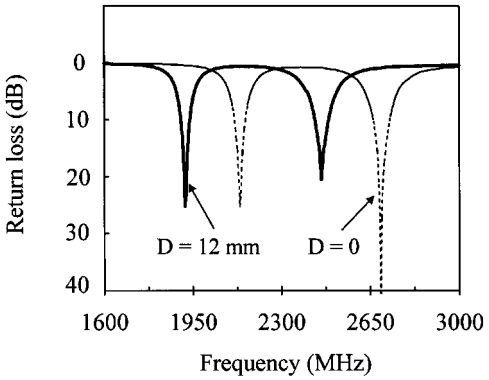


**Figure 3** Return loss versus frequency for the antennas with slot radii of $D = 0$ and 12 mm. Other antenna parameters are given in Figure 2

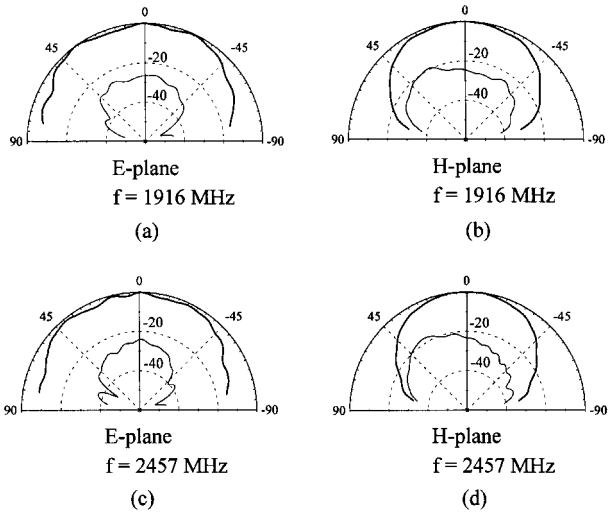


**Figure 4** *E*-plane and *H*-plane radiation patterns at both operating frequencies for the antenna with $D = 12$ mm. Other antenna parameters are given in Figure 3: (a) *E*-plane, $f = 1916$ MHz; (b) *H*-plane, $f = 1916$ MHz; (c) *E*-plane, $f = 2457$ MHz; (d) *H*-plane, $f = 2457$ MHz

As for the radiation patterns at the two operating frequencies, which are of perpendicular polarization planes, no significant variations are found for the antennas with and without a circular slot. Figure 4 presents the radiation patterns for the case of $D = 12$ mm. It is observed that, for both operating frequencies, the radiation patterns are at broadside radiation, and the cross polarizations in the *H*-plane are larger than that in the *E*-plane.

### 3. CONCLUSIONS

The design of a dual-frequency compact rectangular microstrip antenna with a circular slot has been successfully demonstrated. Experimental results have been presented and discussed. Results indicate that, by cutting a circular slot of $D = 12$ mm ($D/W = 0.47$), a 20% antenna size reduction can be achieved, as compared to that of a conventional dual-frequency microstrip antenna [1].

### REFERENCES

1. J. S. Chen and K. L. Wong, "A Single-Layer Dual-Frequency Rectangular Microstrip Patch Antenna Using a Single Probe Feed," *Microwave Opt. Technol. Lett.*, Vol. 11, Feb. 5, 1996, pp. 83–84.
2. Y. M. M. Antar, A. I. Ittipiboon, and A. K. Bhattacharyya, "A Dual-Frequency Antenna Using a Single Patch and an Inclined Slot," *Microwave Opt. Technol. Lett.*, Vol. 8, Apr. 20, 1995, pp. 309–311.
3. C. L. Tang, H. T. Chen, and K. L. Wong, "Small Circular Microstrip Antenna with Dual-Frequency Operation," *Electron. Lett.*, Vol. 33, June 19, 1997, pp. 1112–1113.


CCC 0895-2477/98

# INTEGRATION NETWORK FOR WIRELESS COMMUNICATION AND CATV BROADCASTING WITH FIBER-OPTIC STAR-RING HIERARCHICAL STRUCTURE

**Yang-Han Lee[1] and Jingshown Wu[2]**
[1] Department of Electrical Engineering
Tamkang University
Tamsui, Taipei Hsien, Taiwan, R.O.C.
[2] Department of Electrical Engineering
National Taiwan University
Taipei, Taiwan, R.O.C.

*Received 12 November 1997*

**ABSTRACT:** *In this paper, we make use of the fiber-optic/coaxial CATV network for wireless communications with a star-ring topology to distribute broadcasting cable TV programs and simultaneously to provide bidirectional transmissions for wireless signals. This network utilizes the hierarchical structure with the fiber hub (uplink and downlink both by fiber cable), the semifiberhub (uplink by fiber cable and downlink by coaxial cable), or the coaxial hub (uplink and downlink both by coaxial cable) to increase the system capacity effectively. Three examples, which cover an area of 10 km radius and utilize the GSM scheme, are given: 1) for the single-star ring topology, the system supports 8 hubs and 1000 wireless users; 2) for the multistar ring topology, the system supports 40 hubs and 5000 wireless users; and 3) for the extension topology, the system supports 160 hubs and 20000 wireless users.* © 1998 John Wiley & Sons, Inc. Microwave Opt Technol Lett 18: 132–141, 1998.

**Key words:** *wireless communications; cable TV; fiber optics*

### I. INTRODUCTION

Recently, there have arisen many new challenges for integration of the embedded hybrid fiber-optic/coaxial CATV network to provide wireless communication services and two-way data communication between the subscriber and the head end [1, 2]. A passive optical/coaxial hybrid network for delivery of CATV, telephony, and data services is proposed in [3]. The CATV network utilizes the simulcasting protocol for wireless personal communication [4] and two-way data communication services between the subscriber and the head end, e.g., pay TV, teleshopping, alarm and guard facilities, or interactive videotex [5–7]. Because of the high-speed transmission characteristics of the optical fiber cable, we can eliminate the modulator and demodulator used in the traditional coaxial microcellular system. Therefore, we can design a compact sized and cost-effective antenna tower with an optical fiber microcellular distribution system [8–13].

We propose a star-ring fiber-optic network. This network can distribute broadcasting cable TV programs, and simulta-

neously provide duplex transmission of wireless signals. It employs the star topology for the downlink with direct detection and the ring structure for the uplink with coherent detection. The proposed system has some benefits: 1) it provides wireless bidirectional communication via the existing hybrid optic-fiber/coaxial CATV network; 2) a fiber to the hub system, with $M$ subscribers and $X$ wireless users, shares the same photodetector and phase modulator; and 3) the hybrid fiber-optic/coaxial system is more economical.

*1.1. System Description.* The proposed star-ring fiber-optic network is shown in Figure 1 which employs the star topology for the downlink and the ring structure for the uplink. At the communication head end (as shown in Fig. 2), there are two lasers: one for the downlink with power of $P_D$, and the other for the uplink with power of $P_U$. A $1 \times 2$ coupler is connected to the output of the downlink laser to split the light into two parts. One part is used as the local oscillator for the uplink by coherent detection; the other part is externally modulated by the combined TV and wireless signals, then distributed via a $1 \times N$ star coupler to $N$ hubs. The other laser connects to the ring network to provide an optical carrier to all hubs for uplink signals. At the same time, the optical signal carrying the upstream messages from the other side of the ring is mixed with the local oscillator and detected by the photodetector to recover the messages. Each hub uses a photodetector to detect the TV programs and downlink wireless messages via subcarrier multiplexing (SCM) [14], then distributes the TV programs by coaxial cable to subscribers and wireless messages to a number $X$ of wireless users by antenna. The hub also utilizes a phase modulator to transmit the uplink wireless data from the antenna via the fiber ring network with the cascaded phase modulator scheme [15].

*1.2. Design of the Up–Down Converters.* While transmitting the wireless signals to/from the hub based on the common RF band, we utilize up–down frequency-converting techniques for the transmission of the multiple hubs' wireless signals with the same fiber/coaxial cable between the head end and hubs. In order to transmit the dedicated signals to the destination hub, we use the up–down frequency converter.

There are six different types of up/down converters as shown in Figure 3: Type (A)—$D_{OR}$ down-converts the optical fiber cable spectrum into the RF spectrum, and transmits wireless downlink signals from the photodetector to the antenna via the star fiber network; Type (B)—$U_{RO}$ up-converts the RF spectrum into the optical fiber cable spectrum, and transmits wireless uplink signals from the antenna to the phase modulator for the ring fiber network; Type (C)—$U_{CR}$ up-converts the coaxial cable spectrum into the RF spectrum, and transmits wireless downlink signals from the coaxial cable to the antenna via the coaxial cable network; Type (D) —$D_{CR}$ down-converts the RF spectrum into the coaxial cable spectrum, and transmits wireless uplink signals from the antenna to the coaxial cable for the coaxial cable network; Type (E)—$D_{OC}$ down-converts the optical fiber spectrum into the coaxial cable spectrum, and transmits wireless downlink signals from the photodetector to the coaxial cable for the coaxial cable network; Type (F)—$U_{CO}$ up-converts the coaxial cable spectrum into the optical fiber cable spectrum, and transmits wireless uplink signals from the antenna to the phase modulator for the ring fiber network.

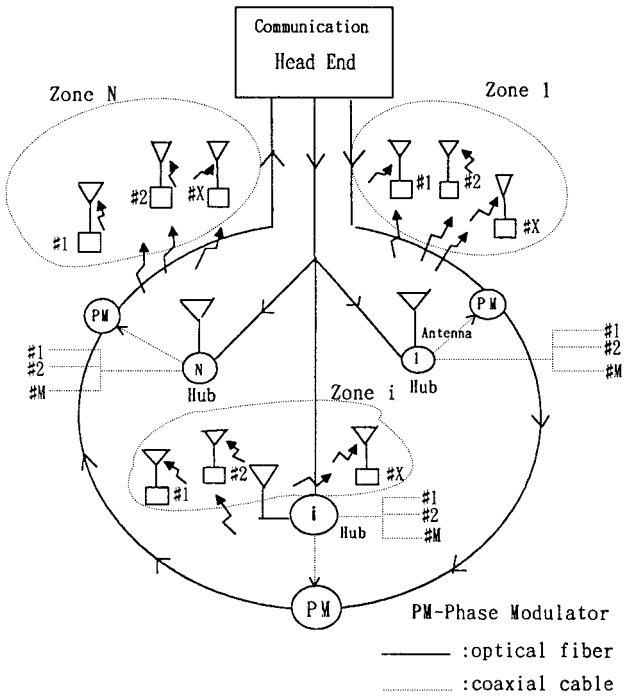


**Figure 1** Schematic diagram of the star-ring fiber-optic CATV network

*1.3. The Hub Structures.* There are four different types of hub structure as shown in Figure 4. Type (A)—Fiber hub (FH) with antenna: Receiving the optical signals from the fiber star network and down-converting the wireless signal with $D_{OR}$ to the antenna, it can also up-convert the wireless signal with $U_{RO}$ to modulate the phase modulator for the fiber ring network. Type (B)—FH as dropper/concentrator: Receiving the optical signals from the fiber star network and down-converting/dropping the wireless signals with $D_{OC}$s to their destination antenna, respectively. It can also up-convert/concentrate the wireless signals with $U_{CO}$s to modulate the phase modulator for the fiber ring network. Type (C)—Semifiber hub (SFH) with antenna: Receiving the RF signals from the dropper of the coaxial cable network and up-converting the wireless signals with $U_{CR}$s to the antenna, it can also up-convert the wireless signals with $U_{RO}$s to modulate the phase phase modulator for the fiber ring network. Type (D)—Coaxial hub (CH) with antenna: Receiving the RF signals from the dropper of the coaxial cable network and up-converting the wireless signals with $U_{CR}$s to the antenna, it can also down-convert the wireless signals with $D_{RC}$s to the coaxial cable network.

*1.4. The Head-End Structure.* The head end receives the downlink wireless signals from the PSTN (Public Switching Telephone Network), and sends them to the corresponding antenna via the fiber star network. The head end collects the uplink wireless signals via the fiber ring network, then transmits them to the PSTN.

*1.5. The CATV-Cellular Structures.* There are two types of CATV-cellular structure. Type (A)—Head end with antenna for wireless cellular communication: In Figure 5(a), we give an example of a CATV-cellular structure with seven cells (one head end together with six hubs). The spacing between antennas is $r$, and the cell radius is $r/2$. Type (B)—Remote

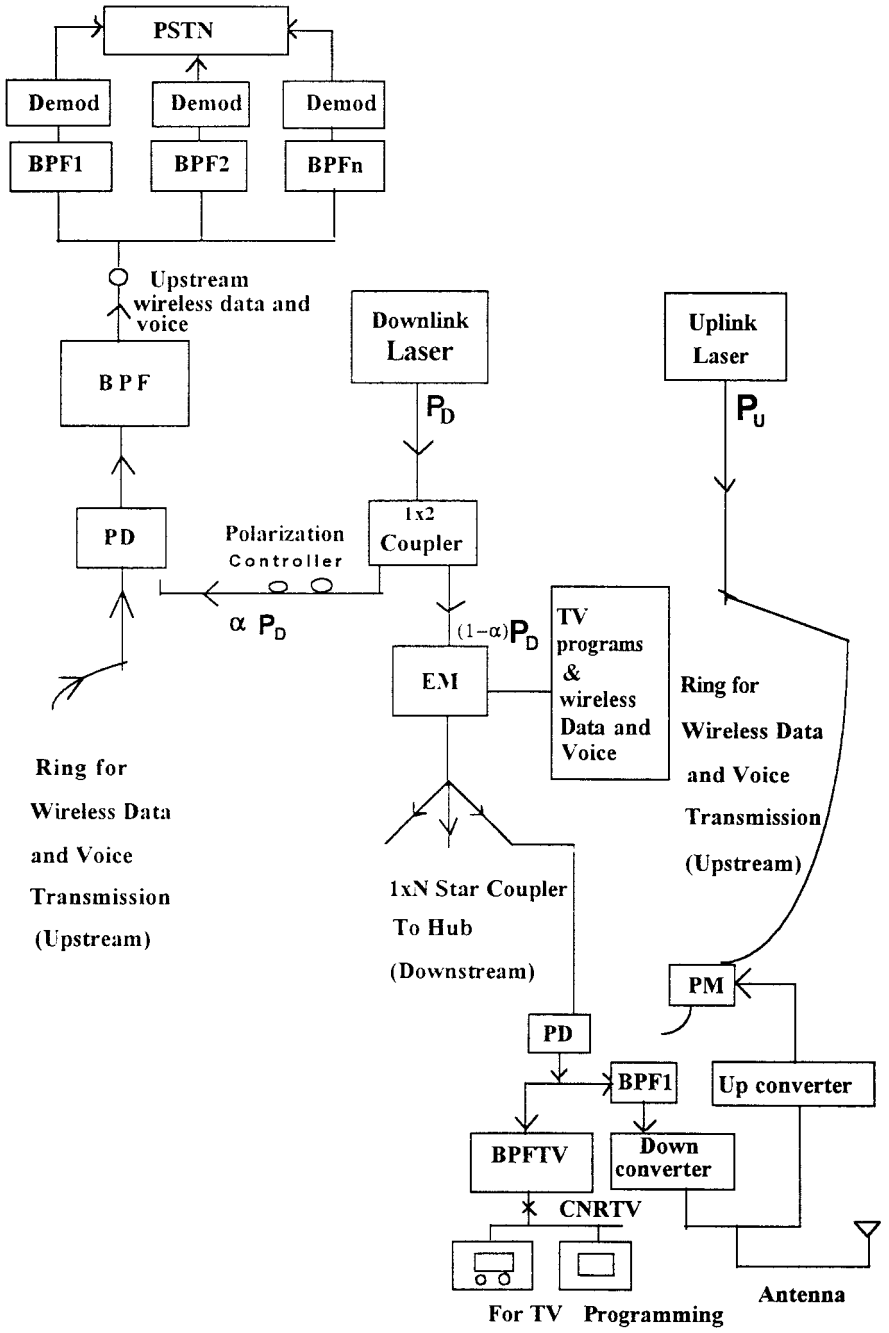


**Figure 2** Communication head-end structure

head end: In Figure 5(b), we have shown the remote head-end CATV-cellular structure where the distance between the head end and the hub can be larger than the cell radius.

*1.6. Design of Hub and Head End.* While transmitting the wireless signals to/from the hub based on the common RF band, we utilize up–down frequency-converting techniques for the transmission of the multiple hubs' wireless signals with the same fiber/coaxial cable between the head end and hubs.

In our network, we may use the fiber hub (uplink and downlink both by fiber cable), the semifiber hub (uplink by fiber cable and downlink by coaxial cable), and the coaxial hub (uplink and downlink, both by coaxial cable) as defined in Figure 4 for four different types of hub structure. Because the fiber hub and the semifiber hub are more expensive than the coaxial hub, we can increase the system capacity in a more economical way.

The head end receives the downlink wireless signals from the PSTN (Public Switching Telephone Network), and sends them to the corresponding antenna via the fiber star network. The head end collects the uplink wireless signals via the fiber ring network, then transmits them to the PSTN.

## 2. ANALYSIS

*2.1. Carrier-to-Noise Ratio for Uplink.* For the uplink, we use the coherent detection as

$$i_U(t) = 2R\sqrt{P_S P_{\mathrm{LO}}}\cos(2\pi f_{\mathrm{IF}} t + \theta_U(t)) \qquad (1)$$

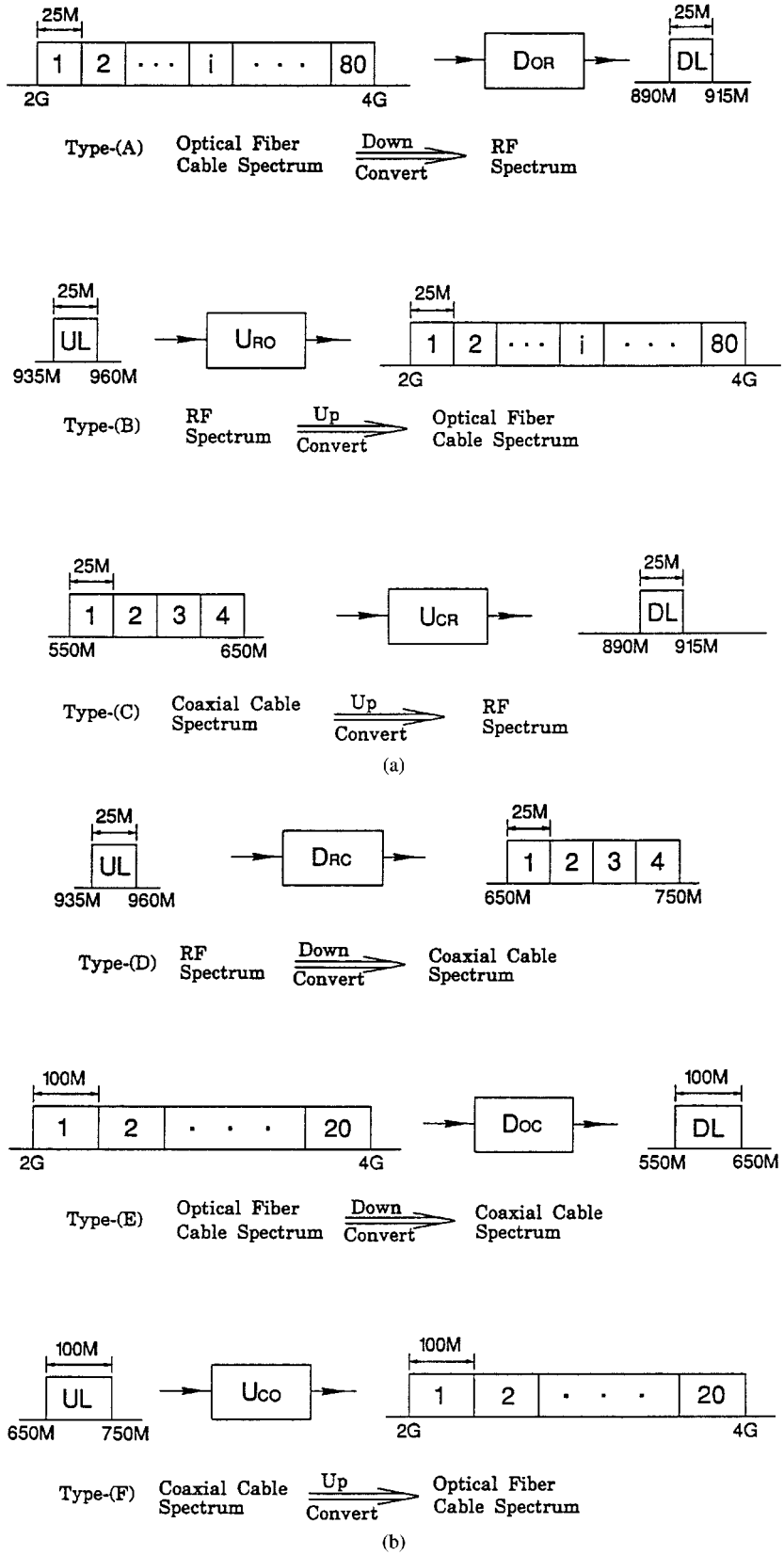


**Figure 3** Different types of up/down converters

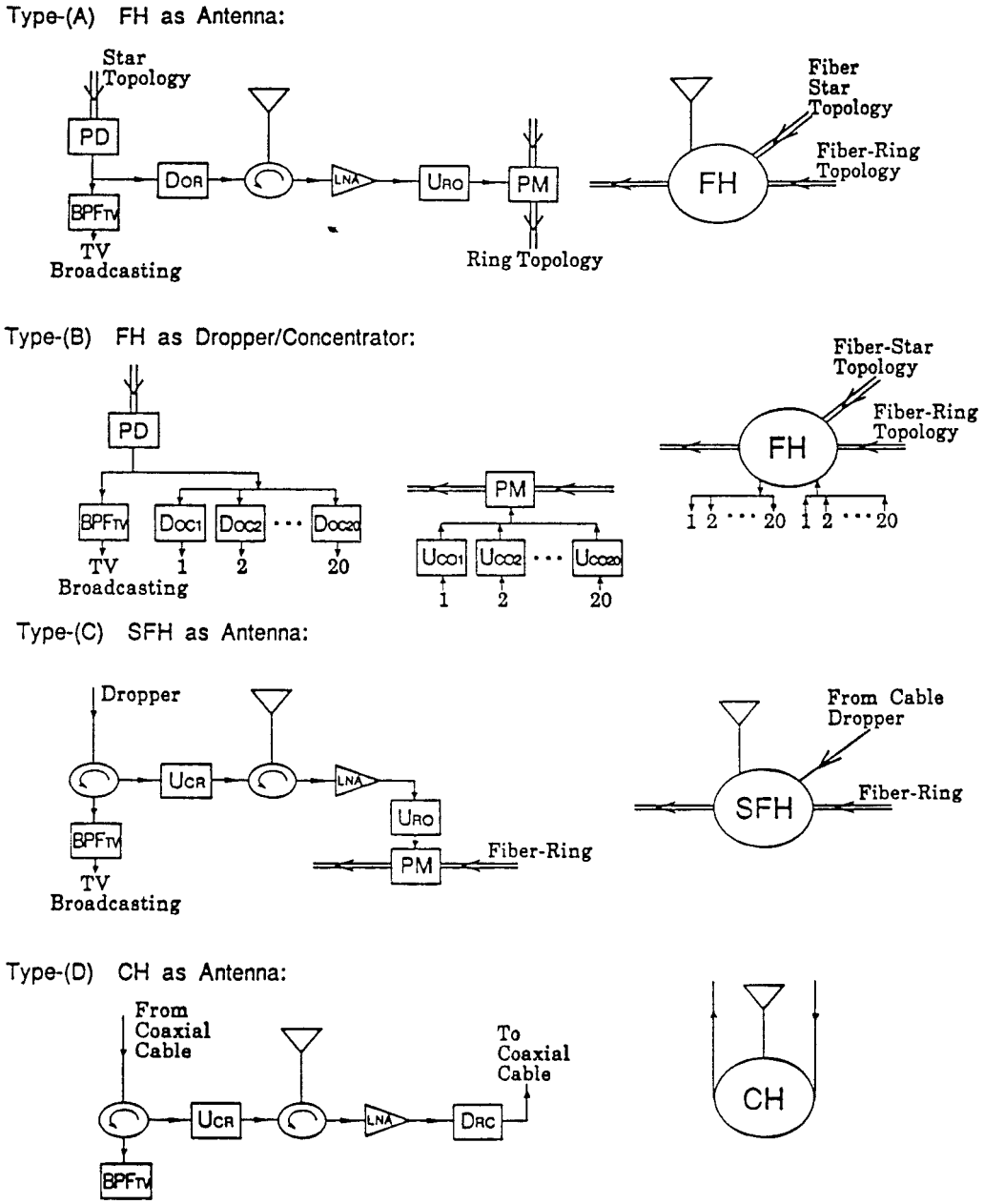


**Figure 4** Different types of hub structure

where $R$ is the responsivity of the photodetector and $f_{\mathrm{IF}}$ is the frequency difference between the downlink and uplink lasers. $P_S$ and $P_{\mathrm{LO}}$ are the received optical signal power and local oscillator power given as $P_S = P_U/(L_{PM}^N L_R)$ and $P_{\mathrm{LO}} = \alpha P_D$, respectively. $\alpha$ is the power ratio of the local oscillator laser over the downlink laser. $\theta_U(t)$ is the uplink wireless signals given as

$$\theta_U(t) = \sum_{i=1}^{N} \sum_{j=1}^{X} \beta_{Ui,j} \sin(2\pi f_{Ui,j} t + \psi_{Ui,j}(t)) \qquad (2)$$

where $\beta_{Ui,j}$, $f_{Ui,j}$, and $\psi_{Ui,j}$ are the modulation index, the subcarrier frequency, and phase for the uplink wireless signals. $10\log_{10} L_{PM}$ is the insertion loss of the phase modulator, assumed to be 3 dB, and $L_R$ is the propagation loss of the uplink fiber for a ring topology, assumed to be $(2\pi r + 2r)\alpha_{\mathrm{fiber}}$ dB, $r$ is the radius between the head end and hub, and $\alpha_{\mathrm{fiber}}$ is the fiber loss.

Assuming that the upstream signals are a single-octave system (for GSM, the system's uplink band is from 935 to 960 MHz), then the carrier-to-noise-ratio (CNR) at the upstream receiver is given by [16]

$$\mathrm{CNR}_U = \frac{0.5R^2 P_{\mathrm{LO}} P_S \beta_U^2}{(\sigma_{\mathrm{sh}}^2 + \sigma_{\mathrm{th}}^2) B_U + h_3 K_3 R^2 P_{\mathrm{LO}} P_S \beta_U^6/32} \qquad (3)$$

where $J_1(\beta_U)$ and $J_0(\beta_U)$ have been given approximately by $\beta_U/2$ and 1, respectively. Thermal and shot noises are given, respectively, by $\sigma_{\mathrm{sh}}^2 = 2eRP_{\mathrm{LO}}$ and $\sigma_{\mathrm{th}}^2 = NFkT/R_L$. $e$ is the electron charge, $B_U$ is the transmission bandwidth for uplink wireless signals, $NF$ is the amplifier noise figure (3 dB), $k$ is Boltzmann's constant, $T$ is the temperature (300 K), and $R_L$

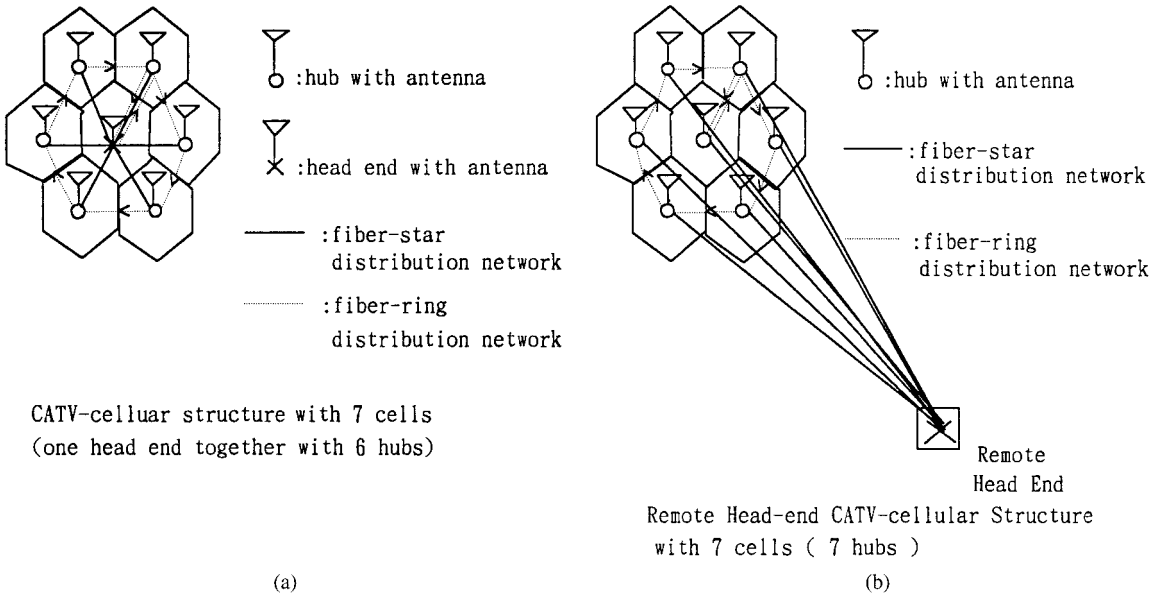


**Figure 5** CATV-cellular structure

is the load resistance. The largest number of the third intermodulation distortion ($IMD_3$), which falls on the central channel [17], is given as

$$K_3 = N_U(N_U/2 + 1)/4 + \left((N_U - 3)^2 - 5\right)/4 \qquad (4)$$

where $N_U = N \times X$ is taken to be even. $h_3$ is the effective factor of $IMD_3$ power within the desired signal band, and is equal to 0.66 [16]. The optimal modulation index for the uplink wireless signal is

$$(\beta_U)_{\text{opt}} = \left(\frac{16(\sigma_{\text{sh}}^2 + \sigma_{\text{th}}^2)B_D}{h_3 K_3 R^2 P_{\text{LO}} P_S}\right)^{1/6}. \qquad (5)$$

*2.2. Carrier-to-Noise Ratio for Downlink.* For the downlink, the detected photocurrent at the hub is given by

$$i_D(t) = RPr(1 + \sin\theta_D(t)) \qquad (6)$$

where $Pr$ is the received dc optical power as $Pr = (1-\alpha)P_D/(L_B L_C L_S)$. $10\log_{10} L_B$ in decibels is the insertion loss of the BBI modulator [18], and $10\log_{10} L_S$ is the propagation loss of the fiber link for star topology. Both are assumed to be 3 dB and $r\alpha_{\text{fiber}}$ dB, respectively. $10\log_{10} L_C$ [dB] is the splitting loss of the $1 \times N$ star coupler, with $L_C$ being equal to $N$. $\theta_D(t)$ is the combined TV programs and wireless signals for the downlink with the total number of $P$ channels and $NX$ wireless users, respectively, as given by

$$\theta_D(t) = \sum_{l=1}^{P} \beta_l \sin(2\pi f_{\text{TV}_l} t + \psi_{\text{TV}_l}(t)) + \sum_{i=1}^{N}\sum_{j=1}^{X} \beta_{Di,j} \sin(2\pi f_{Di,j} t + \psi_{Di,j}(t)) \qquad (7)$$

where $(\beta_l, \beta_{Di,j})$ $(f_{\text{TV}_l}, f_{Di,j})$ and $(\psi_{\text{TV}_l}, \psi_{Di,j})$ are the modulation index, the subcarrier frequency, and the subcarrier phase for the downlink TV and wireless signals, respectively. The modulation indexes for all channels within TV programs and wireless users are chosen to be the same as $\beta_l = \beta_{\text{TV}}$ and $\beta_{Di,j} = \beta_D$, respectively; then the $\theta_D(t)$ is given as

$$\theta_D(t) = \beta_{\text{TV}} \sum_{l=1}^{P} \sin(2\pi f_T V_l t + \psi_l(t)) + \beta_D \sum_{k=1}^{q} \sin(2\pi f_{Dk} t + \psi_{Dk}(t)) \qquad (8)$$

where $q = NX$ and $(f_{Dk}, \psi_{Dk}(t))$ is one-to-one mapped into $(f_{Di,j}, \psi_{Di,j}(t))$. Then we can express $\theta_D(t)$ in terms of a Bessel function extension as

$$\begin{aligned}\sin\theta_D(t) = &\sum_{n_i=-\infty}^{\infty} \cdots \sum_{\sum n_{l_i} + \sum n_{k_i} = ODD} J_{n_{l_1}}(\beta_{\text{TV}}) \cdots J_{n_{l_p}}(\beta_{\text{TV}}) \\ &\times J_{n_{k_1}}(\beta_D) \cdots J_{n_{k_q}}(\beta_D) \sin\{n_{l_1}[\omega_{\text{TV}_1} t + \psi_{\text{TV}_1}(t)] \\ &+ \cdots + n_{l_p}\left[\omega_{\text{TV}_p} t + \psi_{\text{TV}_p}(t)\right] \\ &+ n_{k_1}[\omega_{D_1} t + \psi_{D_1}(t)] + \cdots + n_{k_q}\left[\omega_{k_q} t + \psi_{D_q}(t)\right]\Big]. \end{aligned} \qquad (9)$$

Here, the TV signal band is put away from the wireless signal band; therefore, their cross talk can be ignored. For example, the CATV band is from 50 to 550 MHz, and the downlink of the AMPS system is from 869 to 894 MHz. We use the approximation $J_0(x) \approx 1$ and $J_1(x) \approx x/2$, for $x \ll 1$. For the BBI modulator being biased at the quadrature points such that composite second-order distortion becomes negligible [18], the CNR for downlink wireless and TV signals [16], respectively, is

$$\text{CNR}_D = \frac{R^2 Pr^2 \beta_D^2/2}{\left(\sigma_{\text{sh}}^2 + \sigma_{\text{th}}^2 + \sigma_{\text{RIN}}^2\right)B_D + h_{D3} K_{D3} R^2 Pr^2 \beta_D^6/32} \qquad (10)$$

where $B_D$, $h_{D3}$, $K_{D3}$ and $B_{TV}$, $h_{TV_3}$, $K_{TV_3}$ are the transmission bandwidth, $IMD_3$'s power ratio, and $IMD_3$'s number for downlink wireless and TV signals, respectively. $\overline{\sigma_{sh}^2} = 2eRPr$. $\sigma_{RIN}^2 = RIN\,R^2Pr^2$. RIN represents the relative intensity noise of the laser (here taken as $-165$ dBc/Hz for an Nd:YAG laser [18]). And the $CNR_{TV}$ of TV signals is the same as the above equation, except that we replace the $\beta_D$, $B_D$, $h_{D3}$, and $K_{D3}$ as $\beta_{TV}$, $B_{TV}$, $h_{TV_3}$, and $K_{TV_3}$, respectively. The largest numbers of $IMD_3$s falling on the central channel [16] are given, respectively, as

$$K_{D3} = N_D(N_D/2 + 1)/4 + \left((N_D - 3)^2 - 5\right)/4 \quad (11)$$

$$K_{TV_3} = N_{TV}(N_{TV}/2 + 1)/4 + \left((N_{TV} - 3)^2 - 5\right)/4 \quad (12)$$

where $N_D = N \times X$ and $N_{TV}$ are the number of downlink wireless signals and TV programs, respectively.

And the optimal modulation index for the downlink wireless signals is

$$(\beta_D)_{opt} = \left(\frac{16\left(\overline{\sigma_{sh}^2} + \sigma_{th}^2 + \sigma_{RIN}^2\right)B_D}{h_{D3}K_{D3}R^2Pr^2}\right)^{1/6}. \quad (13)$$

## 3. NUMERICAL RESULTS AND DISCUSSIONS

*3.1. System Parameters.* Considering the system with parameters given as $\alpha = 0.01$, $P_U = P_D = 200$ mW, $N_{TV} = 75$, $r = 1$, 5 km (for the macrocellular and microcellular range from 2 to 5 km and from 0.5 to 1 km, respectively), and $\alpha_{fiber} = 0.4$ dB/km (including the connector loss [19]). In our system, we use two independent lasers and two fiber networks (uplink ring and downlink star) for bidirectional wireless data transmission. Now, taking the GSM system [20, 21] as an example, we have an uplink frequency band from 935 to 960 MHz and a downlink frequency band from 890 to 915 MHz for a channel spacing of 200 kHz. That is, the corresponding system parameters are $X = 125$, $B_U = B_D = 200$ kHz.

The system spectra are shown in Figure 6 as follows. (a) The optical fiber cable spectra for the downlink star network are 50–550 MHz for the 75 TV broadcasting channels, and 2–4 GHz for supporting 80 antenna bands of the downlink wireless signals. Therefore, we need an external modulator with a wide modulation bandwidth from 50 MHz to 4 GHz. (b) The optical fiber cable spectra for the uplink ring network are 2–4 GHz for supporting 80 antenna bands of the uplink wireless signals. Therefore, we need a phase modulator with a modulation bandwidth from 2 to 4 GHz. (c) The coaxial cable spectra for the bidirectional cable network are 50–550 MHz for the 75 TV broadcasting channels, 550–650 MHz for supporting four antenna bands of the downlink wireless signals, and 650–750 MHz for supporting four antenna bands of the uplink wireless signals, Therefore, we need a bidirectional coaxial cable system with a bandwidth from 50 to 750 MHz.

*3.2. Numerical Results*

*A. Single Star-Ring Topology*. We have obtained the total hub number versus the radius between the head end and the hub as shown in Figure 7(a) for a single star-ring topology. For $CNR_U$ larger than 15 dB, the uplink transmission capacity of Type (A), head end with antenna, varies from $N = 2$ ($r = 22$ km) to $N = 20$ ($r = 2$ km), and that of Type (B), remote head end, changes from $N = 2$ ($r = 90$ km) to $N = 20$ ($r = 10$ km). For $CNR_{TV}$ of the downlink with TV signals larger than 50 dB, the downlink transmission capacity is from $N = 2$ ($r = 25$ km) to $N = 20$ ($r = 1$ km), while the $CNR_D$ larger than 15 dB is not the limiting factor.

From Figure 7(b), we notice that there are some different hub numbers between the uplink and downlink, i.e., from $N = 20$ reduced to $N = 8$ and from $N = 18$ reduced to $N = 3$ at $r = 10$ and 20 km, respectively. Therefore, we

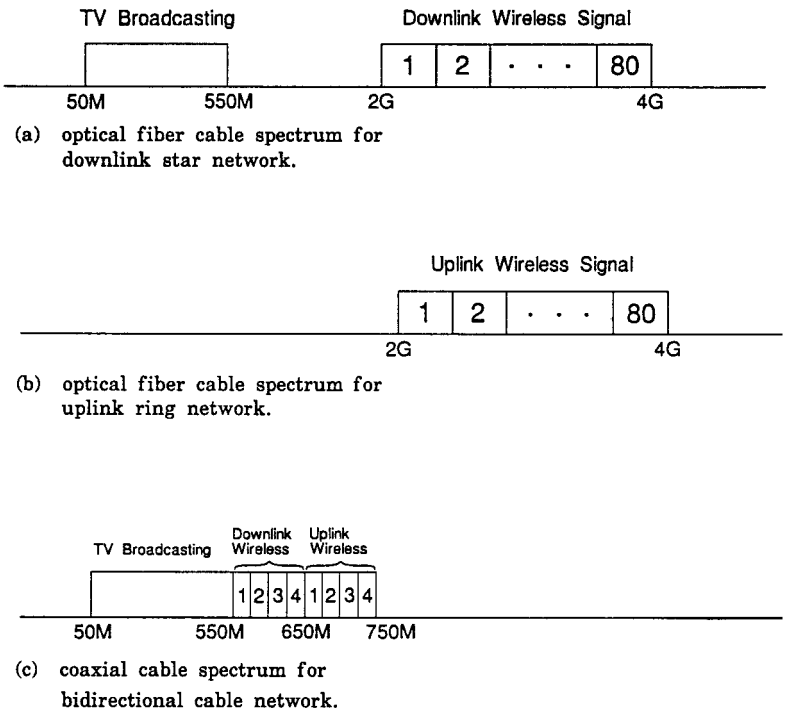


**Figure 6** System spectra

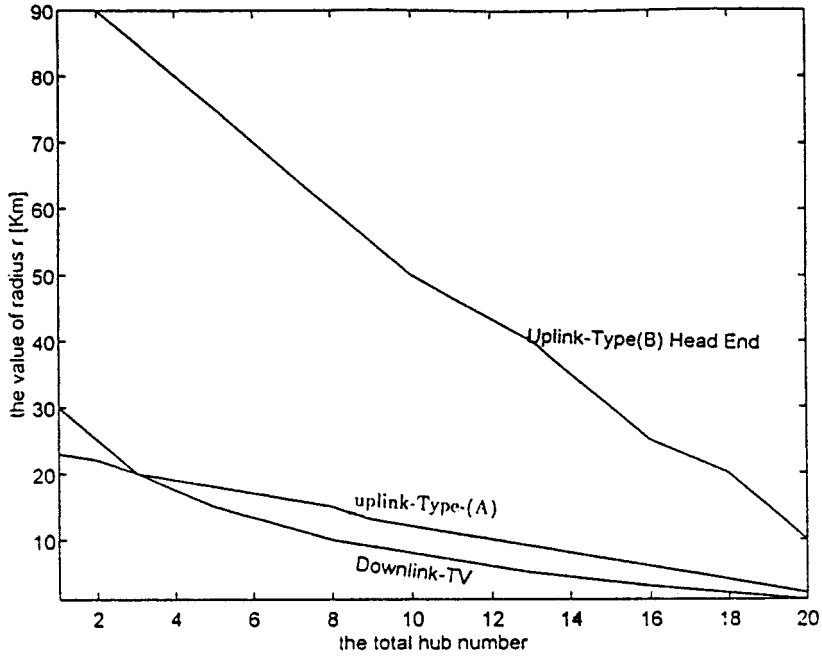


(a)

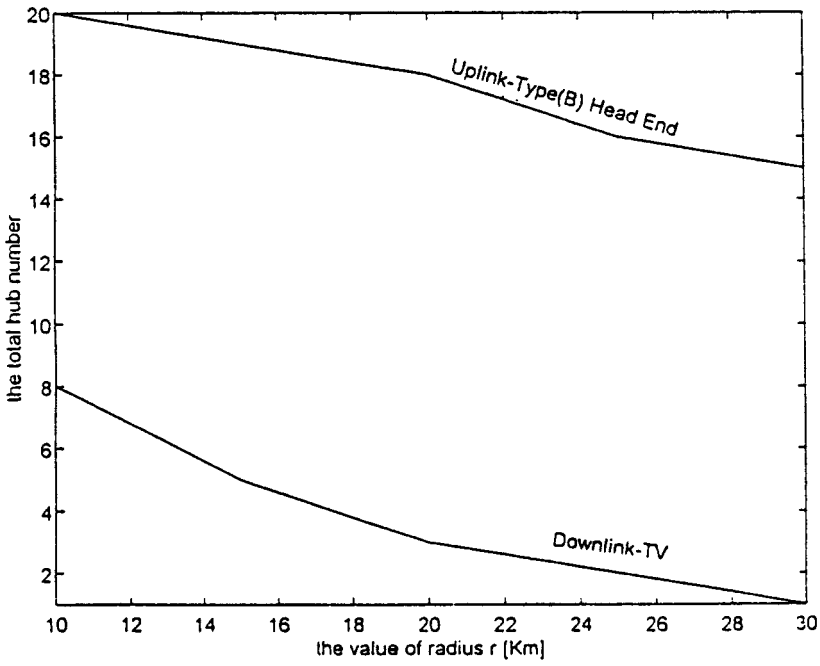


(b)

**Figure 7** (a) Value of radius versus the total hub number for downlink TV, uplink Type (A) head end with antenna, and Type (B) remote head end, respectively. (b) Total hub number versus the value of radius for downlink TV and uplink Type (B) remote head end

propose the multistar-ring and extension system which can utilize the uplink hub to increase the system capacity.

*B. Multistar-Ring Topology*. Some hubs located in the same area may be considered as one group with their corresponding star-ring subnetwork to interconnect the up- and downlinks. In Figure 8, the whole network consists of eight multistar-ring subnetworks. The distance between the head end and the first-level hub (Type (B) FH) is 10 km, while the distance between the first-level hub and the second-level hub (Type (C) SFH) is 0.5 km. The first-level hub receives the optical TV and downlink wireless signals by the photodetector, then distributes those signals to the second-level hub by the coaxial cable. The second-level hubs collect the uplink wireless signals by the fiber ring with the cascaded phase modulators, which are then concentrated at the first-level hubs for transmitting toward the head end by a single pair of fibers. In Figure 8, we use one downlink laser (200 mW) to provide eight Type (B) FHs and two uplink lasers (200 mW), each supporting 20 hubs (four Type (B) FHs and 16 Type (C) SFHs). Therefore, the total hub number is 40, and this

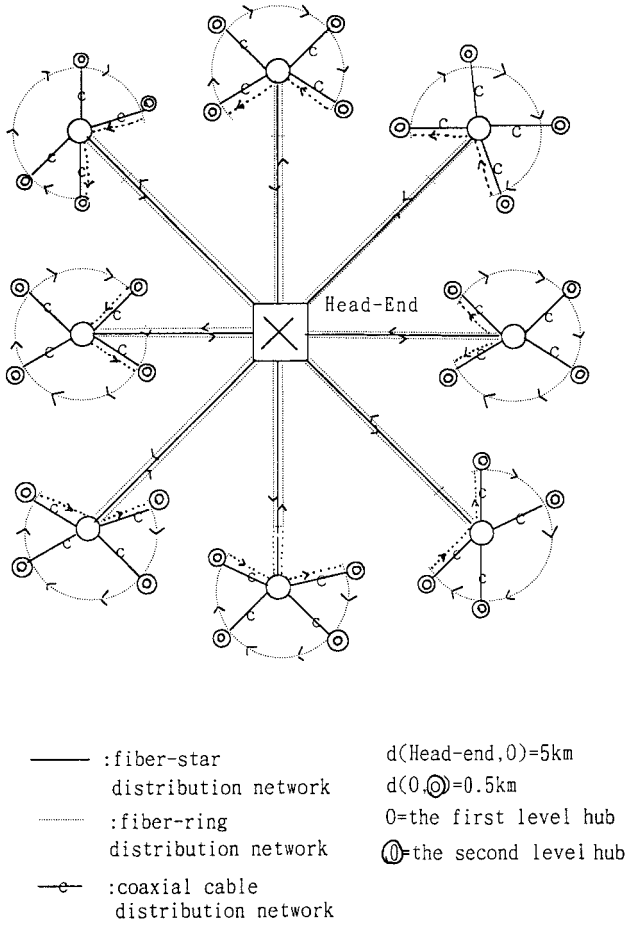


**Figure 8** Multistar-ring CATV cellular structure with $Z = 8$

multistar-ring system can support 5000 ($N = 40$ and $X = 125$) wireless users with a frequency reuse number of 4 for covering an area of radius 10 km.

*C. Extension System*. In our network, we may use the fiber hub (uplink and downlink both by fiber cable), the semifiber hub (uplink by fiber cable and downlink by coaxial cable), and the coaxial hub (uplink and downlink both by coaxial cable) as defined in Figure 4. Because the fiber hub and the semifiberhub are more expensive than the coaxial hub when using a phase modulator for uplink transmission, we can extend the system capacity in this economical way. For example, there are 8 FHs and 32 SFHs in Figure 8.

The performance of the overall system is limited by the downlink TV ($CNR_{TV}$) and the uplink wireless transmission ($CNR_U$) as shown in Figure 7 for the radius of transmission area versus the total hub number. For the downlink TV, the total hub numbers are 20 and 1 FHs within a radius of 1 and 30 km areas, respectively. For the uplink Type (A) head end, the total hub numbers are 21 and 2 FHs within a radius of 1 and 22 km areas, respectively. For the uplink Type (B) head end, the total hub numbers are 20 and 2 FHs within a radius of 10 and 90 km areas, respectively. The Type (B) system outperforms the Type (A) system for considering the location neighborhood.

From Figure 7(b), we can design the extension system with a more systematic method. The difference in the number of hubs between Type (B) and downlink TV is the number of SFHs which can be added in the extension system to increase the total system capacity.

Designing the high-capacity system, we can use the FH as a dropper/concentrator (Type (B) FH) together with the CH as an antenna (Type (D) CH). For covering an area of radius of 10 km, we utilize one downlink laser (200 mW) to provide eight Type (B) FHs and one uplink laser (200 mW) to support eight Type (B) FHs. One Type (B) FH can support 20 Type (D) CHs; therefore, the total number of hubs in this high-capacity system is 160 Type (D) CHs. This system can support 20,000 ($N = 160$ and $X = 125$) wireless users for covering an area of radius 10 km.

The system capacity in terms of the radius of transmission area versus the total hub number is limited by $CNR_{TV}$ of the downlink TV signals and $CNR_U$ of the uplink wireless signals as shown in Figure 7(a). From Figure 7(b), we can design the extension system with a more systematic method. The difference in the number of the hubs between Type (B) and downlink TV is the number of SFHs which can be added to the extension system to increase the total system capacity.

Designing the high-capacity system, we can use the FH as the drop/concentrator (Type (B) FH) together with the CH with the antenna (Type (D) CH). For covering an area of radius to 10 km, we utilize one downlink laser (200 mW) to provide eight Type (B) FHs and one uplink laser (200 mW) to support eight Type (B) FHs. A Type (B) FH can support 20 Type (D) CHs. Therefore, the total hub number in this high-capacity system is 160 Type (D) CHs which can support 20,000 ($N = 160$ and $X = 125$) wireless users.

## 4. CONCLUSION

The proposed star-ring fiber-optic network to distribute broadcasting cable TV programs and simultaneously provide bidirectional transmission of wireless signals is investigated. This system employs the star topology together with an external modulator for downlink direct detection, and a ring structure with cascaded phase modulators for uplink coherent detection. In our network, we may use the fiber hub, the semifiber hub, and the coaxial hub for increasing the system capacity in a more economical way. For the multistar-ring topology, the extension system can support 160 hubs and 20,000 wireless users of the GSM system for covering an area of 10 km.

## ACKNOWLEDGMENT

This work was supported by the National Science Council of the Republic of China under Grant NSC 85-2213-E-032-002.

## REFERENCES

1. D. W. Hardwich, "Integration of Cordless Telephony with CATV Distribution," *ICC'92*, p. 304.3.1.
2. G. Chan and A. Kim, "Measurement of CT-2 Signal Performance Over Cable Television Facilities," *1993 NCTA (National Cable Television Association) Tech. Paper*, San Francisco, CA, pp. 38–46.
3. M. F. Mesiya, "A Passive Optical/Coaxial Hybrid Network Architecture for Delivery of CATV, Telephony and Data Services," *1993 NCTV Tech. Papers*, San Francisco, CA, pp. 358–364.
4. R. W. Donaldson and A. S. Beasley, "Wireless CATV Network Access for Personal Communications Using Simulcasting," *IEEE Trans. Veh. Technol.*, Vol. 43, Mar. 1994, pp. 666–671.
5. H. P. A. van den Boom, "An Interactive Videotex System for Two-Way CATV Networks," *AEU*, Vol. 40, No. 6, 1986, pp. 397–401.
6. M. L. Ellis et al., "INDAX: An Operational Interactive Cable Text System," *IEEE J. Select. Areas Commun.*, Vol. SAC-1, 1983, pp. 285–294.

7. R.j. van der Vleuten et al., "Optional Controlled ALOHA for Two-Way Data Communication in a Cable Television Network," *IEEE Trans. Commun.*, Vol. 42, July 1994, pp. 2453–2459.
8. *IEICE Trans. Commun. (Special Issue on Fiber-Optic Microcellular Radio Communication System and Their Technologies)*, Vol. E76-8, No. 9, 1993.
9. T.-S. Chu and M. J. Gans, "Fiber Optic Microcellular Radio," *IEEE Trans. Veh. Technol.*, Vol. 40, Mar. 1991, pp. 599–606.
10. M. Shibutani et al., "Optical Fiber Feeder for Microcellular Mobile Communication System (H-015)," *IEEE J. Select. Areas Commun.*, Vol. 11, No. 7, 1993, pp. 1118–1125.
11. J. Wu, J. S. Wu, and H. W. Tsao, "A Fiber Distribution System for Microcellular Radio," *IEEE Photon. Technol. Lett.*, Vol. 6, Sept. 1994, pp. 1150–1152.
12. Y. H. Lee, H. W. Tsao, L. P. Chin, and J. Wu, "Wireless Local Communications and CATV Distribution by Using Star-Ring Fiber-Optic Networks," submitted to SPIE, 1995.
13. W. I. Way, "Optical Fiber-Based Microcell Systems: An Overview," *IEICE Trans. Commun.*, Vol. E76-B, Sept. 1993, pp. 1091–1102.
14. R. Olshansky et al., "Subcarrier Multiplexed Broadband Service Network: A Flexible Platform for Broadband Subscriber Services," *J. Lightwave Technol.*, Vol. 11, No. 1, 1993, pp. 60–69.
15. W. Domon et al., "SCM Optical Multiple-Access Network with Cascaded Optical Modulators," *IEEE Photon. Technol. Lett.*, Vol. 5, Sept. 1993, pp. 1107–1108.
16. R. Gross and R. Olshansky, "Multichannel Coherent FSK Experiments Using Subcarrier Multiplexing Techniques," *J. Lightwave Technol.*, Vol. 8, No. 3, 1990, pp. 406–415.
17. M. T. Abuelma'atti, "Carrier-to-Intermodulation Performance of Multiple FM/FDM Carriers Through a GaAlAs Heterojunction Laser Diode," *IEEE Trans. Commun.*, Vol. COM-33, Mar. 1985, pp. 246–248.
18. M. Nazarathy et al., "Progress in Externally Modulated AM CATV Transmission Systems," *J. Lightwave Technol.*, Vol. 11, No. 1, 1993, pp. 82–105.
19. D. M. Fye, "Design of Fiber Optic Antenna Remoting Links for Cellular RF Applications," *Proc. 40th IEEE Veh. Technol. Conf.*, 1990, pp. 622–625.
20. D. Duet et al., "An Assessment of Alternative Wireless Access Technologies for PCS Applications," *IEEE J. Select. Areas Commun.*, Vol. 11, No. 11, 1993, pp. 861–869.
21. D. C. Cox, "Wireless Network Access for Personal Communications," *IEEE Commun. Mag.*, Dec. 1992, pp. 96–115.


CCC 0895-2477/98

# EFFECTS OF COMPENSATION VALUE OF DISPERSION COMPENSATION FIBER ON PRECOMPENSATION SYSTEM

**Jianjun Yu,[1] Kejian Guan,[1] and Bojun Yang[1]**
[1] Beijing University of Posts and Telecommunications
P.O. Box 192
Beijing 100088, P.R. China

*Received 3 November 1997*

**ABSTRACT:** *Employing the nonlinear compensation technology of having dispersion compensation fiber first, the effects of different compensation ratios on the system performance are numerically analyzed. When the input power is large, and the transmission is an amplifier spacing or long transmission distance, the best system performance can be obtained by employing proper undercompensation. Overcompensation and excessive undercompensation are not suitable for long-distance transmission no matter how much the input power is. The larger the input power is, the shorter is the requirement of DCF length.* © 1998 John Wiley & Sons, Inc. Microwave Opt Technol Lett 18: 141–143, 1998.

**Key words:** *dispersion compensation; single-mode fiber; optical fiber communication*

## 1. INTRODUCTION

Dispersion management using dispersion compensation fiber (DCF) is proving to be an efficient technique for upgrading the dispersion-limited performance of embedded standard single-mode fiber (SMF) at high bit rates [1–9]. The performance improvement of having the DCF first was highlighted in [1]. In a bidirectional transmission system, we have to consider the dispersion compensation of having the DCF first. The dispersion management can be classified into: 1) DCF followed by standard SMF (DCF first) and standard SMF followed by DCF (SMF first) according to DCF's position [2]; 2) nonlinear dispersion management or linear dispersion management according to the input DCF power ($\bar{P}_{\mathrm{DCF}}$) [2–4]; and 3) full compensation, overcompensation, and undercompensation according to the dispersion value of DCF [3]. Linear dispersion management has been widely studied [5, 6]. For nonlinear dispersion management, the characteristics of SMF followed by DCF were analyzed in [3]; the results showed that increasing the launching power into the DCF and proper undercompensation led to improving the signal-to-noise rate (SNR). The nonlinear compensation of DCF first and SMF first were compared in [2], where it was found that the optimum channel power can be increased by 6 dB with the DCF first. Different compensation ratios (CR) with the DCF first in nonlinear propagation are compared in this paper. It is found that the best performance can be obtained when proper undercompensation of DCF first is used. The results are similar to the SMF first as in [3].

## 2. NUMERICAL MODEL

We numerically analyze two models as shown in Figure 1. The system configuration in Figure 1(a) includes two erbium-doped fiber amplifiers (EDFA), a 100 km SMF, and 16–18 km DCFs with CR = 0.94–1.06. The fiber's parameters are shown in Table 1. The optical input mean power into the DCF $\bar{P}_{\mathrm{DCF}}$ is chosen as 1, 5, 10, or 15 mW, respectively. The optical input power into SMF $\bar{P}_{\mathrm{SMF}}$ is continually tunable, but $\bar{P}_{\mathrm{SMF}}$ is not smaller than $\bar{P}_{\mathrm{DCF}}$ subtracting the loss of DCF. In Figure 1(b), we consider long-distance transmission. An EDFA, 100 km SMF, and some DCFs are included in each amplifier span. Each amplifier applies a gain $G$ equal to the fiber loss of the following section.

The amplification process is obtained by multiplying the electrical field for the total gain $\sqrt{G_T}$, and by adding to each spectral component of the signal-independent noise terms whose real and imaginary parts are independent Gaussian variables with variance $\sigma^2 = N_{\mathrm{sp}} h\nu(G_T - 1)\Delta\nu/2$, where $N_{\mathrm{sp}}$ accounts for incomplete population inversion ($N_{\mathrm{sp}} = 1$ for complete inversion; $N_{\mathrm{sp}} = 2$ is considered in this work), $h$ is the Planck constant, $\nu$ is the signal carrier frequency, and $\Delta\nu$ is the bandwidth occupied by each Fourier component of the discrete Fourier spectrum.

An optical second-order Butterworth filter (BWF) is used in this work. The transfer function of the optical BWF placed